8-2019

The Structure and Dynamics of a River Delta are Related Through its Nourishment Area, Suggesting Optimality

Christopher A. Cathcart
University of Arkansas, Fayetteville

The Structure and Dynamics of a River Delta are Related Through its Nourishment Area, Suggesting Optimality

A thesis submitted in partial fulfillment
of the requirements for the degree of
Master of Science in Geology

by

Christopher A. Cathcart
University of Wyoming
Bachelor of Science in Geology, 2017

August 2019
University of Arkansas

This thesis is approved for recommendation to the Graduate Council

_____
John Shaw, Ph.D.
Thesis Director

_____
Matt Covington, Ph.D.
Committee Member

_____
Fred Limp, Ph.D.
Committee Member

Abstract

Scaling relations in tributary network geomorphology are well understood with respect to optimality. However, the scaling relations between structure and dynamics in distributary network geomorphology are less well understood. This is primarily due to the fact that nourishment area boundaries are difficult to map compared to tributary network catchment area boundaries. Furthermore, most previous work has focused either on the distributary channel networks or the delta's partitioning of discharge. Here we show that, on the Wax Lake Delta (WLD) in Louisiana, the asymmetry in nourishment areas and downstream nourishment boundary width ($\prod$) at a channel bifurcation, acts as a control upon the partitioning of discharge thereby influencing delta dynamics. We found that relationships between nourishment width, channel width, nourishment area, and discharge can be adequately described by power law functions. Linear power law relationships between discharge and nourishment width show demonstrate a link between a channel network's structure and dynamics. This confirms that individual channel structure is a function of the dynamical competition amongst channels for unchannelized nourishment width and therefore individual channels cannot be considered independently. The uniformity of flux across the downstream nourishment boundary demonstrates the optimality of distribution of water and sediment flux across the unchannelized delta front and suggests self-regulation of the channel structure to achieve maximum entropy of the system. Leave one out cross validation shows that discharge can be predicted with increased accuracy using nourishment width compared to predictions using channel width. This empirically derived scaling relationship will allow for more accurate prediction of discharge partitioning using remote sensing and has important implications for delta geomorphology. These relationships have potential use in future monitoring and management of deltas.

Table of Contents

1 Introduction

River deltas play an important role in human civilization. An estimated 500 million people live on river deltas around the world and many more gain sustenance from their fertile soils (Ericson et al. 2006; Syvitski and Saito 2007). Ancient river delta systems include substantial energy reservoirs of both oil and natural gas (Rainwater 1966; Ericson et al. 2006). Due to a combination of rising sea levels and the damming of many river systems, many deltas are going from progradation to retrogradation (Ericson et al. 2006; Edmonds et al. 2011; Foufoula-Georgiou et al. 2011). Distributary channel networks are the primary control on the distribution of water and sediment across the delta (Tejedor et al. 2017). Primary channels distribute water and sediment through the system and into the receiving basin while secondary channels connect the primary channels to the inundated island interiors (Shaw, Mohrig, and Whitman 2013). The partitioning of water and sediment through the channels within the network determine channel erosion and deposition as well as delta front evolution (Van Heerden and Roberts 1988; Wellner et al. 2005). The coupled channelized and unchannelized system set the structure of the delta. The dynamics are set by the concomitant partitioning of discharge across a downstream nourishment end boundary. Using a combination of remote sensing and field data, this study seeks to empirically characterize the scaling relationships between the structure and the dynamics of the Wax Lake Delta (WLD) in coastal Louisiana.

Distributary channel networks have obvious equivalents in the tributary river networks that supply them, as both are dendritic structures which transport water and sediment. In tributary networks, scaling relationships have been discovered which connect channel hydraulics, catchment area, and the principle of optimality, the concept that systems will self-regulate to minimize energy expenditure (MEE) and maximize entropy production (MEP). Therefore,

comparing the scaling relationships found in distributary networks to those found tributary networks could provide insight into the geomorphology of distributary networks.

The foundational scaling relationships found for the hydraulics of tributary channels were presented by Leopold, Wolman, and Miller [1964]. They empirically derived power law scaling relationships between a channel's width, depth, velocity, and discharge. (1)

$$w = aQ^b \; d = \; cQ^f \; u = kQ^m \;\; Q = aQ^b \cdot cQ^f \cdot kQ^m \qquad (1)$$

$$where \; b + f + m = 1 \; and \; a \cdot c \cdot k = 1$$

where *w* is channel width, *d* is channel depth, *u* is velocity, *Q* is discharge, and *a,b,c,f,* and *m* are constants which vary depending on network characteristics such as bank cohesiveness and sinuosity.

Analysis of the empirical data led Leopold, et al [1964] to conclude that discharge increases much faster than depth of water in a channel. These scaling relations not only furthered our understanding of channel hydraulics and geomorphology they also provided a means for predicting discharge from satellite imagery. Gleason and Smith [2014] measured channel widths from remote imagery and used the scaling relationship between channel width and discharge to approximate discharge rating curves for continental scale riverine systems. Verification, using gauging stations, of the calculations for reach-averaged discharge found root-mean-square error of 20-30%(Gleason and Smith 2014).

Hack [1957] found an empirical scaling relationship between the area of a drainage basin, designated as A, and the length of its longest channel, L. (2)

$$L = 1.4(A)^{0.6} \qquad (2)$$

The area of the drainage basin is the average width of the drainage basin, $\overline{w}$, multiplied by the length of the longest channel so that $A = \overline{w} \cdot L$.

Substituting into equation 2,

$$L = 1.4\ (\overline{w} \cdot L)^{0.6}$$

$$L^{1.66} = 1.75(\overline{w} \cdot L) \qquad (3)$$

The ratio of average width to length,

$$\frac{\overline{w}}{L} = 0.57/L^{0.33} \qquad (4)$$

The ratio of width to length, therefore, increases inversely as the third power of the length and must decrease as the length increases. As a catchment area grows in the downstream direction it becomes longer and narrower as the channel length increases. The larger the basin the more elongate it is demonstrating that the overall shape of the drainage basin is geometrically connected to the geometry of the tributary network (Hack 1957).

Horton [1945] used the hydraulic mechanics of infiltration capacity, transmission capacity, and Manning's formula to derive the rational equation of peak discharge from a drainage basin which relates discharge in a tributary network and its catchment area. (5)

$$Q = ciA \qquad (5)$$

where Q is peak discharge, c is a runoff coefficient based upon ground cover, i is rainfall intensity and A is catchment area.

This equation shows the relationship between catchment area and discharge in tributary networks and is a principle equation in many landscape evolution models.

The scaling relationships found in tributary networks have been related to the system's optimality. Rodriguez-Iturbe et al. [1992] theorized a connection between energy dissipation, runoff production and the structural characteristics of tributary networks to explain their geomorphology. After comparing digital elevation maps of tributary networks to optimal channel network configurations they found ratios of bifurcations, channel length, and catchment area in agreement with Hack's scaling relationships. This was found to imply that the tributary channel network self-organized to minimize energy expenditure of the flow through the system (Rodríguez-Iturbe et al. 1992).

In distributary channel networks, scaling relationships for channel hydraulics are relatively well understood. Mikhailov [1970] empirically investigated distributary channel hydraulic relationships at bankfull discharge of the Volga, Danube, Kura, Amu-Darya, and Terek deltas. Andén [1994] empirically investigated the hydraulic geometry relationships found in the Laitaure Delta, Swedish Lappland. Both Mikhailov and Andén found that the scaling relationships between channel width, depth, velocity, and discharge in deltaic environments to be compatible to the scaling relationships found by Leopold et al. [1964] albeit with marginally varied constants. These results imply that the fluid dynamics for channelized tractional flow remain consistent even under conditions of backwater flow.

Edmonds, et al. [2011] established the quantitative metric of nourishment area to differentiate and evaluate diverse delta systems. The nourishment area is a specific area of the delta which is supplied by sediment from a given channel cross section. This is analogous to the catchment area in tributary networks. Edmonds [2011] found that nourishment area scales well with channels length because as length grows the nourishment area also grows congruently. This finding disagrees with the elongation of catchment area seen in Hack's law. Hack [1945] found

the ratio of width to length in drainage basins increased inversely to the third power of the length.

Relatively few studies have included the unchannelized system when analyzing distributary channel networks. As the channelized flow moves basinward, the flux from the primary channels into the secondary channels and inundated island interiors increases due to friction and shallowing of the channels (Hiatt and Passalacqua 2015). The lateral out flow results in a significant amount of flux (23-54%) escaping the channels into the unchannelized area (Shaw, Mohrig, and Wagner 2016; Hiatt and Passalacqua 2015). This substantial amount of flux using unchannelized pathways necessitate that the unchannelized region be considered when analyzing the dynamics of a distributary network system. Ke et al [2019] showed that distributary channel growth can be entirely understood by this outflow.

The study of scaling relationships in distributary networks remains limited because the nourishment boundaries cannot be derived from topography, unlike tributary systems in which unchannelized flow patterns are generally inferred from the gradients of topography (Passalacqua et al. 2010, 2015). However, biofilm streaklines provide a means of estimating the unchannelized flow patterns on deltas. Biofilm streaklines have been used to track sub-mesoscale sea surface flow fields (Johannessen et al. 1996; Seppke, Gade, and Dreschler-Fischer 2013). As streaklines are tangential to flow direction the resulting geometries can provide a synoptic view of the flow patterns (Shaw, Mohrig, and Wagner 2016). Two assumptions are necessary for this method to be accurate. First that the streakline patterns do not vary significantly through relevant timescales. Second, that the resulting flow direction are a function of depth averaged flow and not secondary flow patterns. For the purposes of this study we used streakline derived flow as a means of delineating the nourishment boundaries.

Another complicating factor in the study of scaling relationships in distributary networks is the fact that downstream nourishment boundary can be theoretically placed anywhere from the shoreline to far into the receiving basin. For the purposes of this study we define the downstream nourishment boundary of the area as a line of equipotential head. If this head is relatively large, the line is proximal, if this head is relatively small the line is relatively distal. For ease in evaluating connections between delta structure, dynamics, and optimality we introduce the nourishment area end boundary width as a metric unto itself (∏) (Figure 1). The placement of this boundary is of vital importance because the state of the flow field at the chosen distance greatly effects the nourishment area and nourishment width. It will be shown that proximal placements of nourishment width are at regions where the flow is out of equilibrium with the receiving basin as it is transitioning from confined to unconfined flow. This results in nourishment area and nourishment width measurements which are not representative of the discharge.

Optimality in distributary channel systems has been analyzed in terms of maximum entropy production (MEP). Entropy in distributary networks is the measure of uncertainty in the pathways of the water and sediment flux or in other words the degree of diversity of flux distribution across the delta (Tejedor et al. 2017). A distributary network with low entropy would consist of one primary channel conveying the predominance of the flux whereas a distributary network with high entropy would be composed of multiple primary channels creating numerous potential pathways.

Tejedor et al. [2017] represented the distributary channel network geometry of 10 field and 6 Delft3D deltas as nodes and links to analyze the uncertainty of the flux pathways compared to 10^5 randomizations of flux partitioning to analyze the nonlocal entropy rates of the deltas. While

none of the deltas were perfectly optimal all were found to have a nonlocal entropy rate above the 90th percentile. This demonstrated that the coevolution of the structure of the distributary channel network and the flow dynamics allows for the delta to self-regulate in an attempt to optimally distribute water and sediment uniformly across the shoreline (Tejedor et al. 2017).

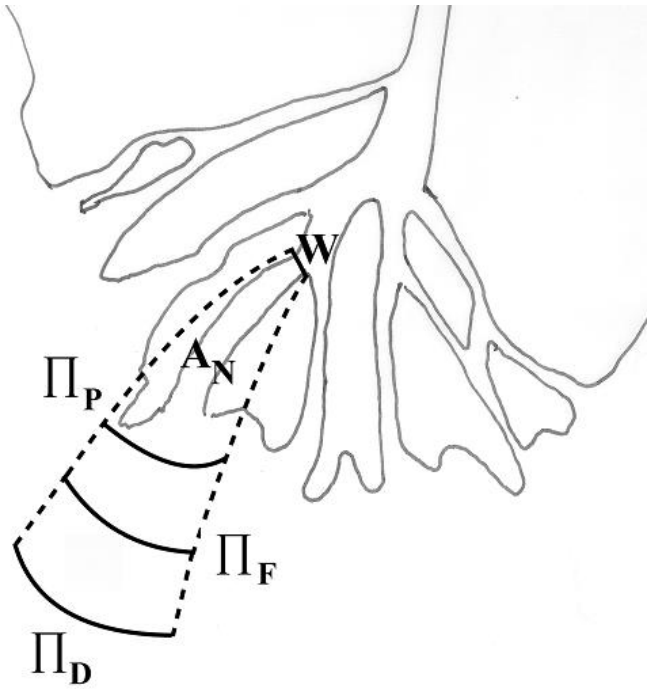

Figure 1: A conceptual diagram showing the measured components with downstream nourishment width mapped at 3 equipotential surfaces. The dotted lines are nourishment boundaries that may be derived from streaklines, W is channel width, and $\prod_P$ is nourishment width proximally, $\prod_F$ placed at the delta front, and $\prod_D$ placed distally. Nourishment area A_N is the area between W, nourishment boundaries, and a downstream boundary width.

The goal of this study is to characterize the scaling within the coupled channelized and non-channel system by measuring nourishment width, channel width, discharge, nourishment area, and sediment fluxes in the WLD. In order to assess these connections between individual channel components and the unchannelized area we (1) quantify the partitioning of discharge across the delta by using cross sectional velocity profiles collected at asymmetrical bifurcations

and connecting them to their measured nourishment area and nourishment width (2) compare the empirically derived scaling relationships to comparable relationships found in tributary networks, (3) validate the empirically derived scaling relationships, given the colinear nature of the measured components leave one out cross validation will be used for prediction model validation, (4) investigate the related time scales of the metrics, and (5) compare the integrated results from the above with current theories related to optimality. The conclusions drawn from these analyses will further our understanding of the geomorphology of prograding river dominated deltas.

2 Site Description

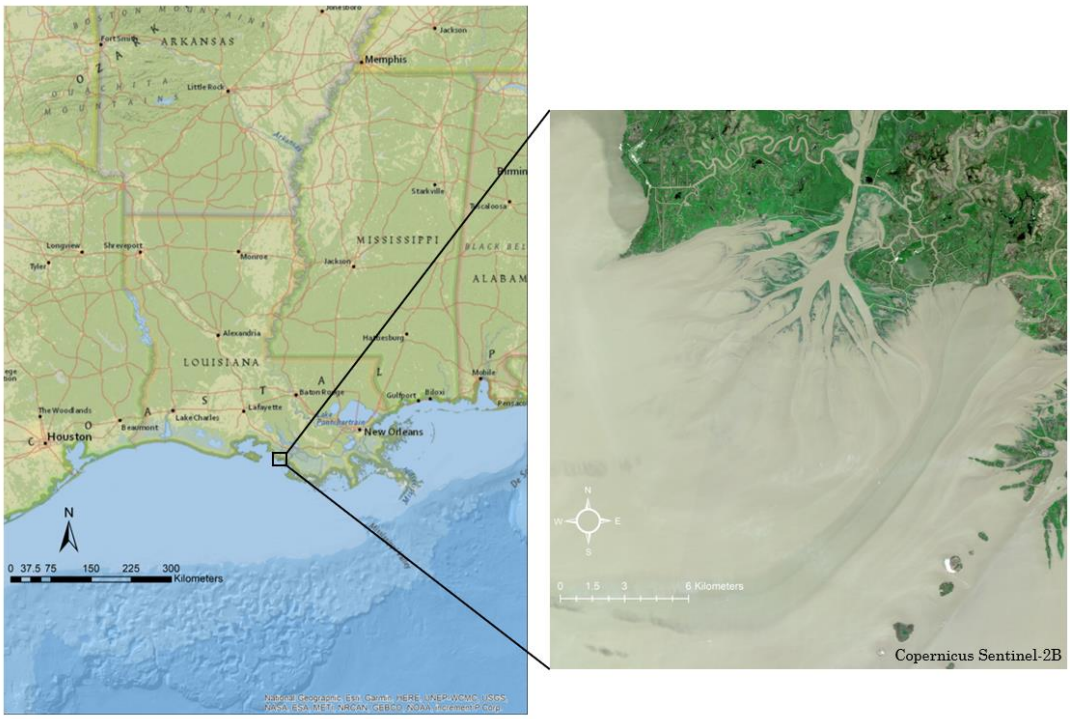

Figure 2: a) Map of Louisiana with the research area highlighted. (Sources: National Geographic, Esri, DeLorme, HERE, UNEP-WCMC, USGS, NASA, ESA, METI, NRCAN, GEBCO, NOAA, iPC) **b)** Sentinel 2 image acquired March 22, 2018. Note the streaklines present on the delta front.

Located in coastal Louisiana the Wax Lake Delta (WLD) is approximately 150 km southwest of New Orleans (Figure 2). The result of dredging by the Army Corps Of Engineers in 1942, the

WLD receives 40% of the flow discharge from the Atchafalaya River (Hiatt 2013).In 1973, the WLD became subaerial exposed and has continued to prograde into the Atchafalaya Bay (Roberts et al., 1997). The geometry of the distributary channel system on the WLD is a bifurcating network of seven primary channels and multiple secondary channels with few loops. Beyond the subaqueous delta front the topology of the bed becomes predominantly uniform (Shaw et al. 2016; Whaling, 2019). The sheltered nature of the Atchafalaya Bay, in which the WLD is located, allows for the streaklines composed of floating biofilms, coming from the vegetated unchannelized regions, to remain coherent. The presence of these streaklines is required for our method of mapping nourishment area and nourishment width. The WLD was chosen as the research area for this study because of its progradational nature, geometry of the distributary channel system, and the existence of streaklines. As it is one of the few places located on the Louisiana coast which is land is growing it is an ideal place to study the geomorphology of a growing delta. The rarity of loops within the distributary channel structure and the sheltered nature of the bay ensure that measurements of discharge taken at channel cross sections are an accurate reflection of the partitioning of discharge.

3 Methodology

The methodology for this study was composed of analysis of empirical data obtained from remote sensing and field work on the WLD. Added to this data was empirical data collected by Hiatt (2013).

Remote Sensing

Channel widths, nourishment widths, and nourishment areas were calculated in ArcMap using Sentinel 2, acquired March 22, 2018, and Landsat 5 TM, acquired November 2, 2011, images of the WLD (Figure 3a and 3b). The NIR band for each image (Sentinel 2 Band 8 and Landsat 5

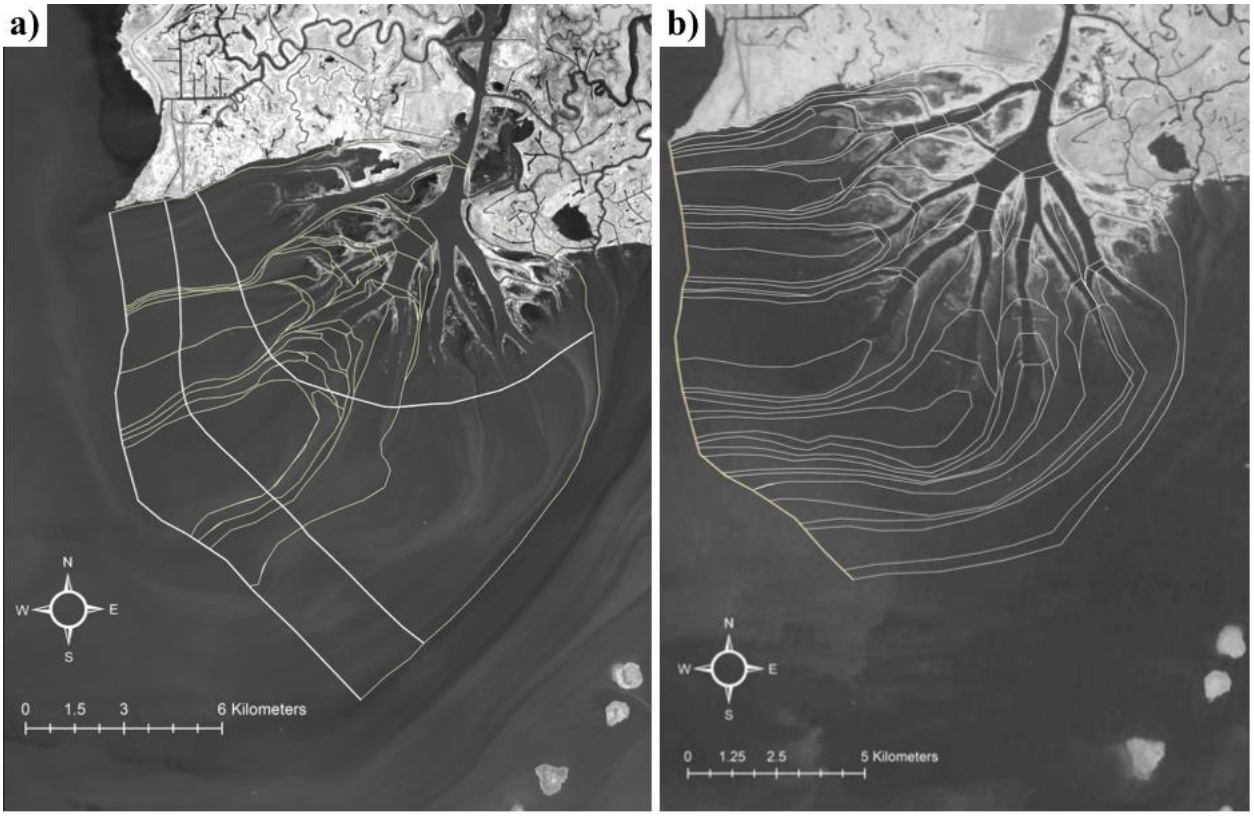

Figure 3: a) Sentinel 2 image T15RXN_20180322T163939 Band 8 (acquired March 22, 2018) with nourishment areas mapped with the downstream nourishment boundary placed at 3 equipotential surfaces, $\prod_P$ is nourishment width proximally, $\prod_F$ placed at the delta front, and $\prod_D$ placed distally. **b)** Landsat 5 image LT05_L1TP_023040_20111102_20160830_01_T1 band 4 (acquired November 2, 2011) with nourishment areas mapped with downstream nourishment boundary placed at same location as 2018 $\prod_D$.

Band 4) were chosen for mapping purposes because of well-defined channels and levies and streaklines allowing for easier measurements. In cases of links created by a secondary channel connecting with another primary channel, the nourishment area and width were mapped as a commensurate slice of the receiving primary channel's nourishment area, based on our reasoning that the disproportionally smaller contribution of the secondary channel would be entrained in the primary channel. In contrast to the method used by Edmonds et al. (2011) which included the entire receiving primary channel's nourishment area. Channel width remote imagery measurements for the 2018 data were validated in the field.

Biofilm streaklines were used for delineation of the boundaries between nourishment areas. A flow net was constructed by using the streaklines as flow lines and then constant head lines were demarcated by inscribing lines perpendicular to the flow lines. Nourishment area and the nourishment width were then calculated using ArcMap.

Errors and Accuracy

Manually digitizing nourishment area boundaries inherently introduces error into final measurements. These errors include: 1) resolution and accuracy of the remote image, 2) the accuracy and precision of placed polygon boundaries, 3) potential variability of using a streakline as a synoptic tracer for flow.

Carisio (2012) defined total surface area error, E as a combination of total measurable uncertainty, E_1, and potential variability error, E_2:

$$E = E_1 + E_2 \qquad (6)$$

$$E_1 = \sqrt{A} + (p + u) + \sqrt{2} \qquad (7)$$

$$E_2 = A * v \qquad (8)$$

Where A is area of the polygon, p is the horizontal uncertainty of the source image, u is the horizontal uncertainty, and v is potential variability error.

Imagery errors depend on the source of the image. The horizontal position error for both Sentinel 2 and Landsat TM 5 images is ≤ 12 m (Wiedermann et al. 2014; Borgeson, Batson, and Kieffer 1985). Horizontal accuracy of polygon boundaries placed along streaklines is a function of the scale of the map created and can be quantified by using standards employed by the United States Geological Survey's National Mapping Program standards (USGS 2017). For the purposes

of this study, the horizontal accuracy was calculated, using the USGS standards, to be 16.94 meters for the Sentinel 2 and 20.33 meters for the Landsat 5 image by using the scale at which the features were mapped. For the purposes of this study, and to account for all other potential errors, a relatively high 5% value was used for potential variability error.

Field Data

Discharges were measured by doing quadruplicate transects at each parent and daughter channel of 13 asymmetrical bifurcations using a boat mounted Teledyne RiverPro Acoustic Doppler Current Profiler collected from March 20 to March 23, 2018. This study also used discharge data collected by Hiatt [2013] from February 04 to February 07, 2012, which measured a substantial portion of the delta including the same bifurcations measured in 2018.

Data Analysis

Nourishment width, channel width, nourishment area, and discharge data were compiled and then analyzed to assess the relationships between the partitioning of discharge, nourishment width, and nourishment area. Owing to the colinear nature of the components, Leave One Out Cross Validation (LOOCV) was used for discharge prediction model validation. LOOCV is a technique by which a data point is removed from the dataset and then its value is predicted using the remaining data for a given metric. This is then repeated for every data point in the data set and the predicted values are then compared to the actual values (Johnson and Wichern 2007).

4 Results

Normal hydraulic geometry relations predict that channel width and depth will scale with discharge. When $w = aQ^b$ $d = cQ^f$ $u = kQ^m$ the 2018 data for the WLD show a = 9.56 ±5.73, b = 0.514 ±0.08, c = 0.338 ±0.043, f = 0.33 ±0.065, k = 0.299 ±0.043, and m = 0.162 ±0.021 (± 1

standard error). These results are comparable with results from past studies of both tributaries and other bifurcating deltas implying that scaling relationships for channel discharge, width, depth and velocity are consistent in both tributary and distributary networks.

Regression analysis of the scaling relationship between nourishment area with a distal downstream boundary and the discharge of a given channel cross section demonstrated a quasi-linear relationship with scaling exponents of 1.05 ± 0.039 for 2012 and 1.082 ± 0.017 for 2018 (Figure 4). Discharge measured at the USGS gauging station 07381590 for the Wax Lake Outlet at Calumet, LA was 7080 cubic meters per second during the 2018 fieldwork and 4250 cubic meters per second during the 2012 fieldwork. The ratio between incoming discharge at Calumet between 2012 and 2018 is 0.6 and the ratio of the scaling law coefficients for the dataset's regression (0.53) are comparable (Figures 4). With identical placement of the end boundary, under varying flow conditions, and six years apart the distribution of discharge remains comparable while the absolute discharge varies. The similar regression fittings show that the linear relationship displayed in the data is related to the proportionality of the flow and not of the absolute flow. To normalize the discharge, the values were dividing by the associated discharge measurement at the gaging station at Calumet. To normalize the nourishment area and nourishment width, the values were divided by the nourishment area and width of the entire delta with the end boundary placed distally (Figure 3a). The scaling relationship between the normalized values demonstrate an equivalent quasilinear relationship and more clearly reveals the relationship between distribution of nourishment area and the partitioning of discharge (Figure 5).

The measured nourishment areas, and therefore the results, were dependent upon the selection of the downstream end boundary of the nourishment area (Figure 1). In this study we measured

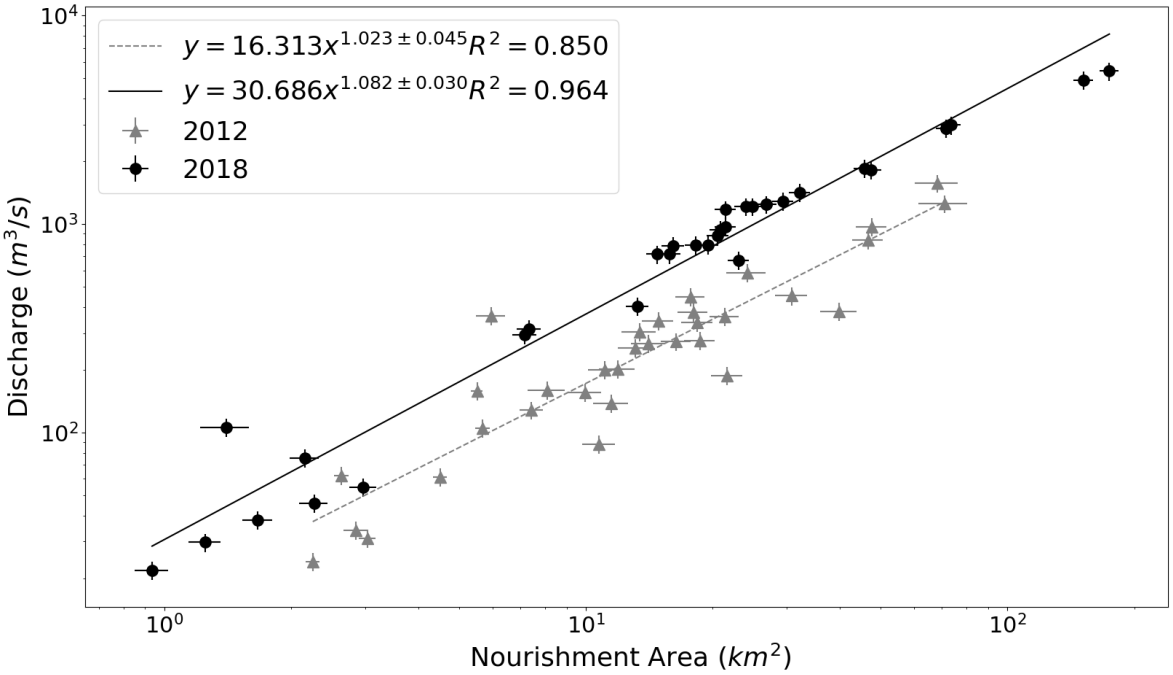

Figure 4: Comparison of Nourishment Area with Nourishment Width placed distally and Discharge with power law fits for the Wax Lake Delta in 2012 and 2018. Nourishment areas are mapped in Figures 3 and 3b.

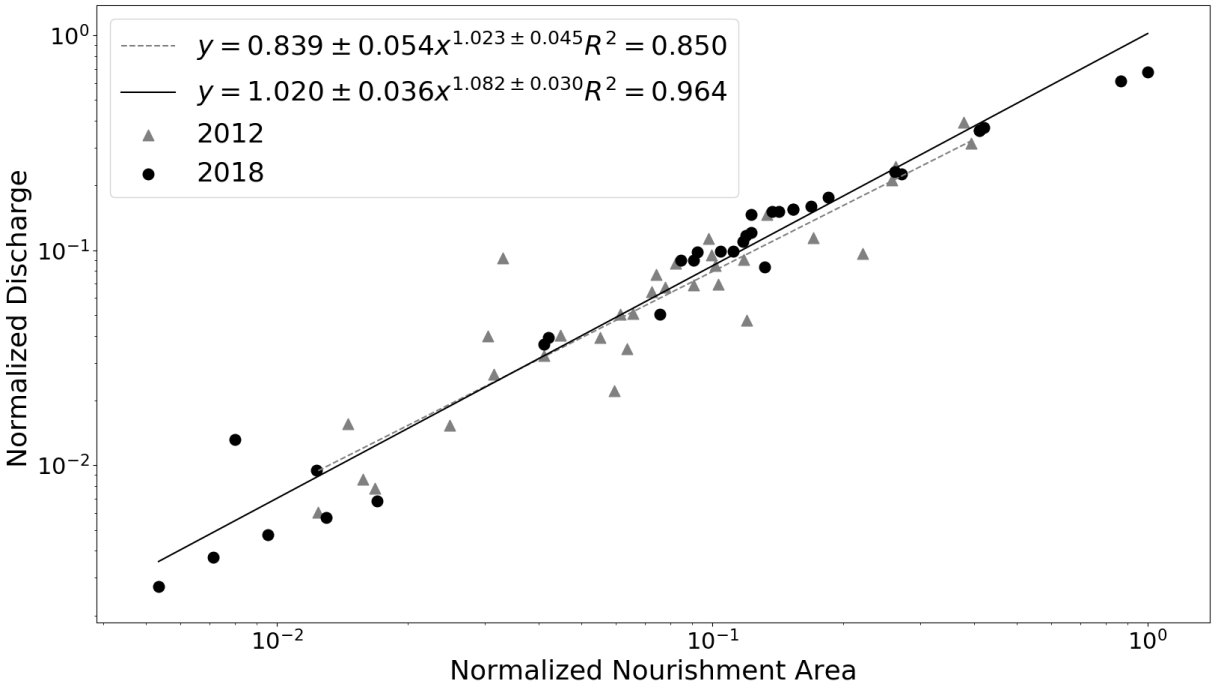

Figure 5: Comparison of normalized Nourishment Area with Nourishment Width placed distally and normalized Discharge with power law fits for the Wax Lake Delta in 2012 and 2018.

nourishment areas for the 2018 data with the downstream nourishment boundary defined at three nourishment areas for the 2018 data with the downstream nourishment boundary defined at three locations: the shoreline, the subaqueous delta front, and at an equipotential surface beyond the subaqueous delta front. (Figure 3a) The empirically derived scaling relationship was influenced by the end boundary placement (Figure 6). Proximal placement of the end boundary resulted in an exponent less than one with a greater standard deviation and a low coefficient of determination. Placement at the delta front resulted in a quasi-linear scaling relationship with a lower standard deviation and a significant coefficient of determination. Distal placement resulted in similar quasi-linear power law scaling and a marginally higher coefficient of determination.

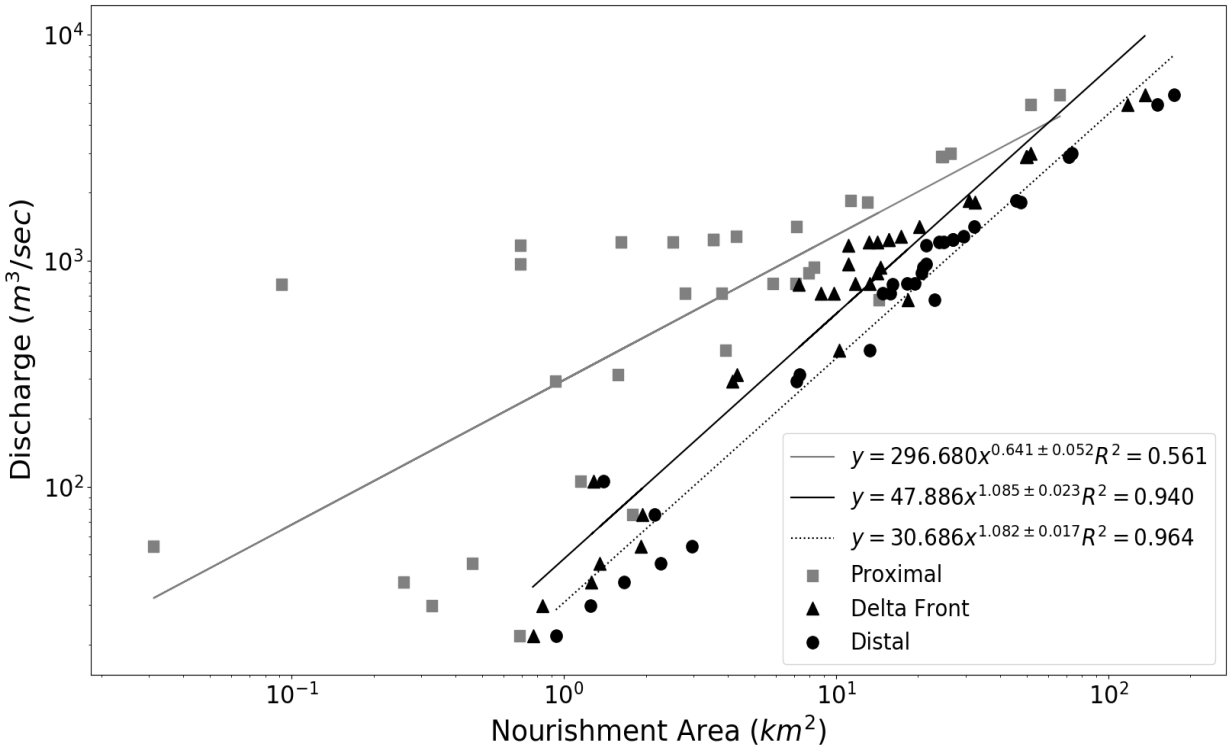

Figure 6: Comparison of Nourishment Area with Nourishment Width placed proximally, at the delta front, and distally and Discharge with power law fits for the Wax Lake Delta in 2018. Nourishment areas are mapped in Figures 3a.

Regression analysis of the scaling relationship between nourishment width with a distal downstream placement and the discharge of a given channel cross section demonstrated a comparable quasi-linear relationship with scaling exponents of 0.989 ± 0.058 for 2012 and 1.071 ± 0.027 for 2018 (Figure 7).

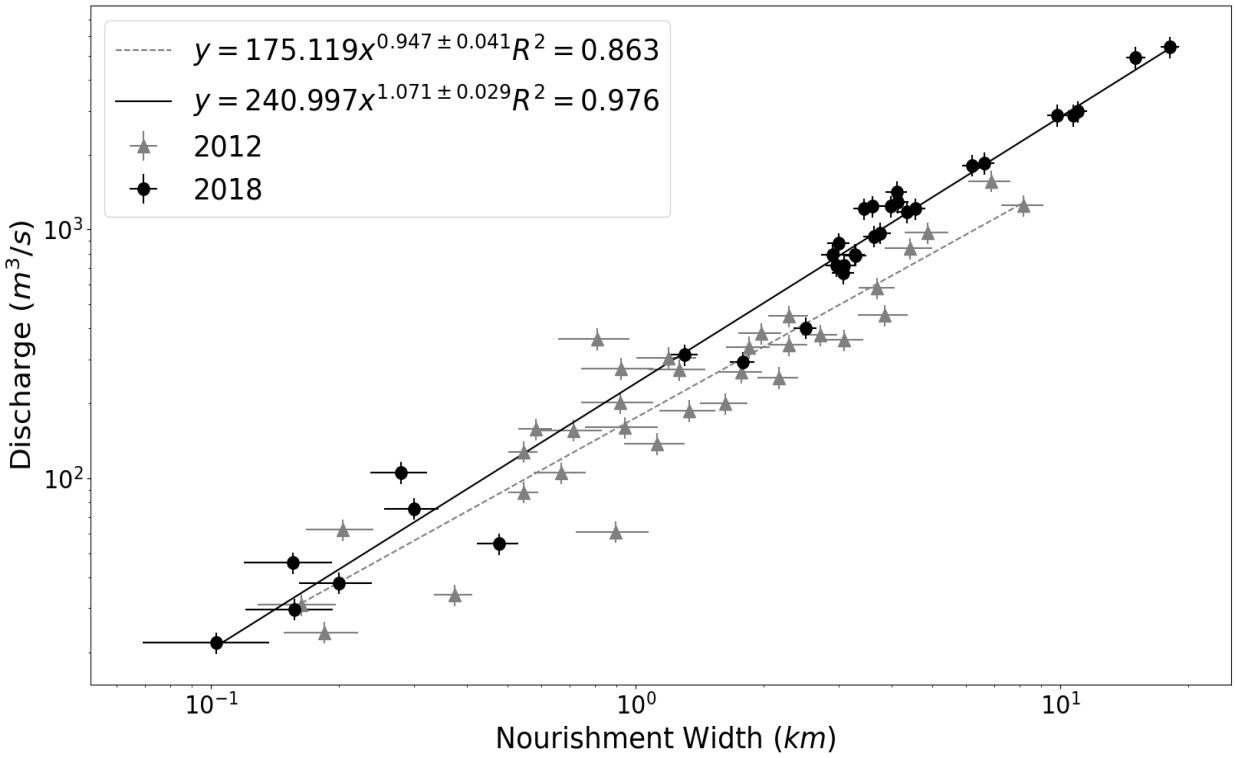

Figure 7: Comparison of Nourishment Width and Discharge with power law fits for the Wax Lake Delta in 2012 and 2018. Nourishment widths are mapped in Figures 3a and 3b.

Similarly, the relationship for normalized data demonstrates the connection between proportion of the nourishment width and proportion of discharge (Figure 8). Analysis of the 2018 nourishment widths, with the downstream nourishment boundary defined at three locations: the shoreline, the subaqueous delta front, and at an equipotential surface beyond the subaqueous delta front, departed from the nourishment area data showing quasi-linear relationships at all placements (Figure 9).

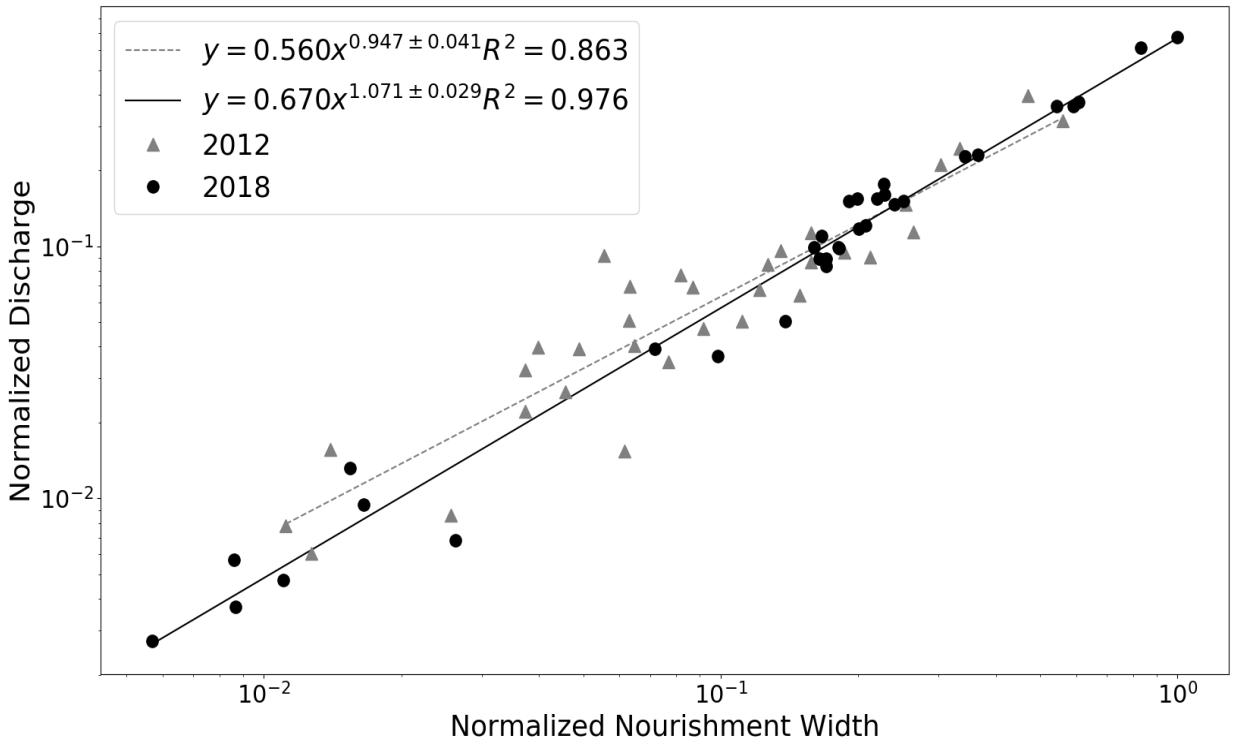

Figure 8: Comparison of normalized Nourishment Width and normalized Discharge with power law fits for the Wax Lake Delta in 2012 and 2018.

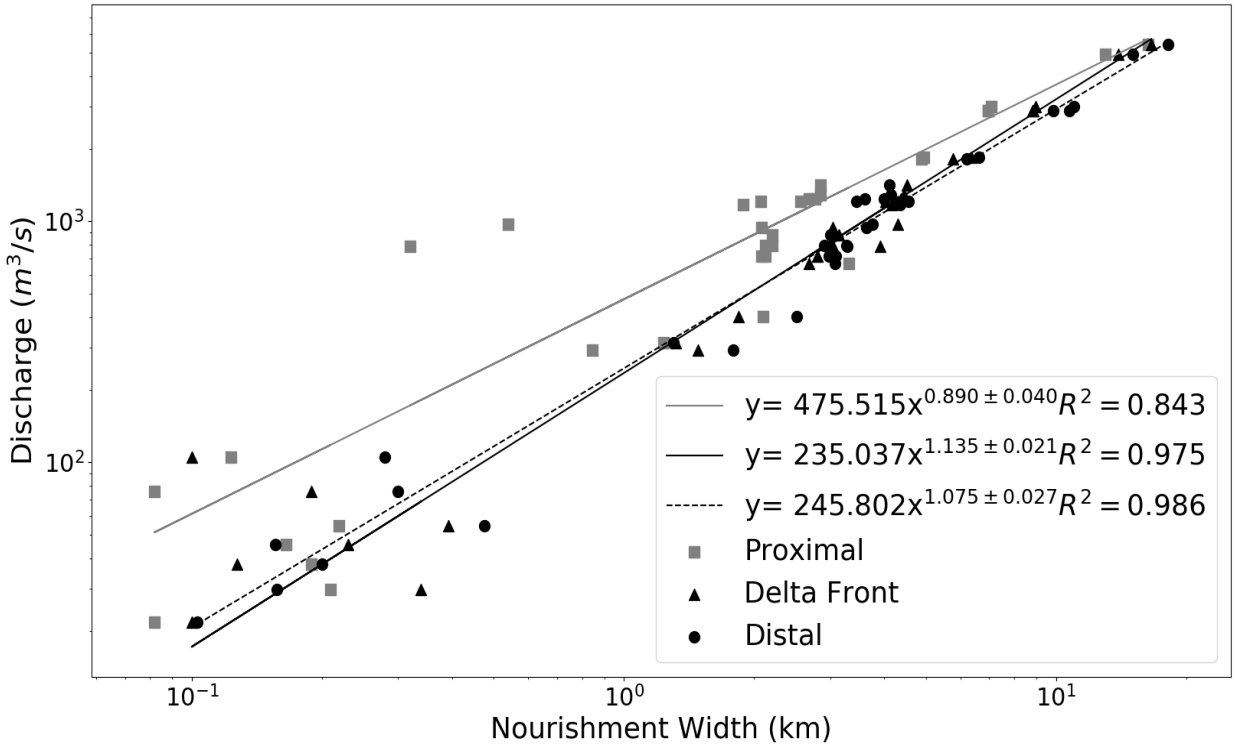

Figure 9 Comparison of Nourishment Width with Nourishment Width placed proximally, at the delta front, and distally and Discharge with power law fits for the Wax Lake Delta in 2018. Nourishment widths are mapped in Figures 3a.

Then, for the 2018 data, we divided discharge by nourishment width to evaluate the flux across nourishment width proximally, at the delta front, and distally (Table 1). Proximal placement produces a substantial standard deviation with a large coefficient of variability signifying the disequilibrium of the hydraulics with this equipotential line as the flow is transitioning from confined to unconfined flow. The mean showed a decrease in flux per meter of nourishment width as the standard deviation diminished and the coefficient of variation decreased with distance. An equipotential surface with maximum entropy production would be perfectly evenly distributed, i.e. Coefficient of variation would be zero. These trends demonstrate the evolution of the flow as it approaches an equipotential line of MEP.

Table 1: Discharge (Q) of a given transect divided by Nourishment Width (∏) placed proximally, at the delta front, and distally for the Wax Lake Delta in 2018.

	Q / Proximal ∏(m^2/s)	Q / Delta Front ∏(m^2/s)	Q / Distal ∏(m^2/s)
Mean	0.505603	0.293229	0.262881
Standard Deviation	0.451242	0.147725	0.057432
Coefficient of Variation	0.892484	0.503787	0.218472

We used Leave One Out Cross Validation (LOOCV) to compare the predictive strength of channel width, nourishment area, and nourishment width for water discharge. The resulting predictions are then compared to the actual values. This prediction model validation for discharge prediction indicates that, for the Wax Lake Delta, nourishment width is the best predictor of discharge with nourishment area being essentially equivalent while channel width was found to only be a fair predictor (Figure 10).

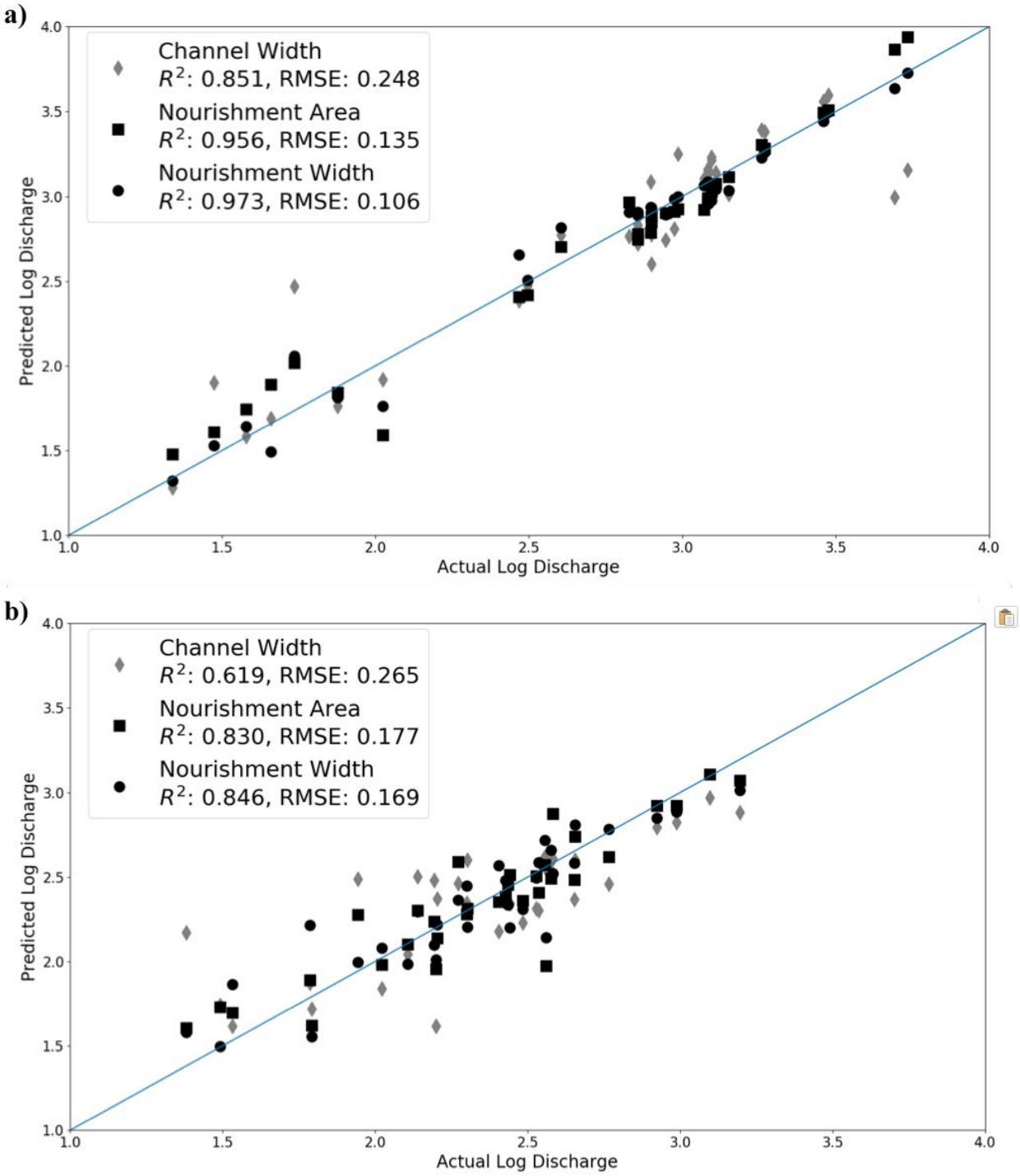

Figure 10: Results of the LOOCV for predicting Discharge on the Wax Lake Delta using Channel Width, Nourishment Area, and Nourishment Width using **a)** 2018 data and **b)** 2012 data. Note the values are the log of discharge.

5 Discussion

Optimality

When nourishment width was evaluated at a proximal equipotential line the scaling relationship between discharge and nourishment area was found to be non-linear (Figures 6 and 9). However, the scaling relationship between discharge and nourishment area were found to be quasi-linear with placement of nourishment width at equipotential lines located distally or at the delta front. We interpret the change in scaling behavior from proximal to distal equipotential surfaces to be associated with a transition from highly variable flux along a surface to quasi-uniform flux along a surface. As the relatively high velocity flows from the primary channels transition from confined to unconfined flow there is significant lateral flow expansion due to friction and shallowing of the channels. As the relatively low velocity flows from the secondary channels and unchannelized areas transition there is contraction of flow as the velocity increases.

At a sufficient distance, downstream the bed topography is predominantly uniform(Shaw et al. 2016; Whaling 2019). We propose that at this distance the combination of uniform topography, flow expansion, flow contraction, friction, and the low bed slope result in the water surface slope becoming virtually uniform and subsequently the flow velocity becomes quasi-uniform. The combination of uniform velocity and consistent depth results in the discharge per unit length being quasi-uniform along this equipotential line. The uniformity of the downstream nourishment boundary, under dynamic conditions found at this equipotential line implies that this is a curvilinear sink for the point sourced input discharge. This is comparable to tributary networks were the line sourced discharge enter the point sink of the downstream channel.

Optimality, in tributary systems, is evaluated in terms of MEE because the potential energy can be measured anywhere in the system using the water surface slope. While MEE cannot be

directly measured in distributary systems, it is possible to measure discharge and discharge partitioning which allows for optimality in distributary systems to be assessed in terms of MEP. Furthermore, given the principle that deltas grow due to the distribution of fluxes across the delta top, through channel network evolution, rather than a single pathway it is more appropriate to calculate distributary networks in term of MEP. In terms of MEP the equipotential line is where the flux has attained its dynamically accessible maximum entropy rate. The entire water and sediment flux distributed by the system is divided equally per unit length of the nourishment width for the entire delta, creating an equal probably of pathways.

Structure and Dynamics

Here we show how the nourishment area connects the structure and the dynamics of the WLD. Deltas are extremely dynamic systems with topology and discharge partitioning coevolving. The delta's topology sets the structure of the delta. The dynamics are set by the discharge partitioning across a downstream nourishment boundary width which determines channel erosion and deposition as well as delta front evolution. The power law scaling relationships show the interconnection between a channels discharge, nourishment area, and nourishment width (Figures 5 & 8). The scaling relationships between the structure and the discharge partitioning of the WLD were seen to be consistent under conditions of two discharges and six years apart, indicating that these relationships are consistent for the WLD. If these power laws adequately describe partitioning on the WLD, connections between the structure and dynamics can be illustrated with two thought experiments. First, we can imagine a dynamic change as an increase in discharge down a particular distributary channel with associated decrease in the remainder of the network. This channel's width, depth, velocity, nourishment area and boundary width would also increase and cause lateral shifts of nourishment boundaries.

These increases would result in decreases of proportion of discharge, nourishment area, and boundary width of adjacent channels and in turn the entire network, thus changing the structure. Second, changes to a channels structure would result in changes to its discharge and to the partitioning of discharge across the delta. So, it could be imagined that if a channel were to receive a greater fraction of the discharge it's width, depth, velocity, nourishment area and boundary width would also increase. These increases would result in decreases of proportion of discharge, nourishment area, and boundary width of adjacent channels and in turn the entire network. Equally, changes to a channels structure would result in changes to its discharge and to the partitioning of discharge across the delta.

These scaling relationships, if applicable elsewhere, could improve remote sensing analyses of inaccessible deltas. Currently the calculation of discharge of inaccessible deltas is done by analyzing satellite imagery to measure channel widths (Kraaijenbrink 2012). The widths were then used in conjunction with Leopold's channel hydraulic scaling relationships to calculate discharge. The results of this study imply that, for remote deltas which have conditions such that nourishment areas and boundary widths can be mapped through streaklines (such as the Mackenzie Delta in the Northwest Territories, Canada), discharge and discharge partitioning can be better predicted using either nourishment area (85.2%) or nourishment width (92.7%) compared with discharge predictions using channel width (68.3%) (Figure 10).

The interconnection between morphodynamical changes and nourishment area has several implications including using remote sensing to deduce dynamic changes from nourishment changes and controlled diversion management. Drastic changes in the deltas structure in response to perturbations, such as avulsions dredging, choking, and abandonment of channels

would be reflected in changes to all of the nourishment areas and nourishment area end boundary widths of the entire delta.

Lastly, the results have interesting implications for the management of controlled sediment diversions that are planned in coastal Louisiana (CPRA 2012). For example, deepening or widening a channel through dredging would cause an increase of discharge which would alter the distribution of nourishment areas and discharge partitioning. By analyzing overall discharge partitioning of a delta and then altering it, while considering how it would influence the rest of the network, it would theoretically be possible to control the position of areas of deposition and erosion. Thereby, influencing conservation, growth, and loss of land on the delta.

Nourishment Width and Nourishment Area

Nourishment area was found to scale linearly with discharge (Figure 4). In tributary settings, the relationship between catchment area and discharge is the result of uniform precipitation (a spatially distributed source) over a catchment area and is a central and easily justified assumption in many landscape evolution models (Equation 5). In contrast water leaves deltas through the uniform equipotential line that acts as a curvilinear sink at the downstream boundary that is optimized to uniform water flux (Table 1). While a linear scaling relationship between discharge and nourishment width is physically justified (see Optimality), the relationship between discharge and nourishment area need not hold. This is demonstrated by the non-linear scaling relationship between nourishment area and discharge with a proximal end boundary (Figure 6).

We use geometric reasoning to justify the linear scaling between discharge and nourishment area found when the nourishment width is placed at the delta front or distally. The channel width, nourishment width, and the length of the nourishment boundaries form a shape that can be

closely approximated with a quadrilateral. Therefore, the nourishment area can be approximated by:

$$A_N = \left(\frac{W + \prod}{2}\right) * L \qquad (9)$$

Where A_N is nourishment area, W is channel width, $\prod$ is nourishment width, and L is length of the nourishment boundaries

The channel widths range from 35-885 meters whereas nourishment width ranges from 200-18,100 meters and are predominantly at least an order of magnitude larger that the given channel width. Therefore, as the channel width is insignificant compare to the nourishment width, we can disregard channel width and equation 6 becomes:

$$A_N = \left(\frac{\prod}{2}\right) * L \qquad (10)$$

The length of the side boundaries was found to have little correlation with discharge (r^2 =0.48) due to the fact that, aside from the apex, there are asymmetrical bifurcations at all distances of the channel network and therefore for a given length there can be greatly varying discharges. Therefore, we can disregard length of the nourishment boundary and equation 7 becomes:

$$A_N = \left(\frac{\prod}{2}\right) \qquad (11)$$

As we have seen that discharge(Q) scales with nourishment width we can substitute that into equation 11:

$$A_N = \left(\frac{\mathrm{Q}}{2}\right) \qquad (12)$$

Thus, we propose than a channels nourishment area is set primarily by its nourishment width resulting in an equivalent quasi-linear scaling relationship.

Time Scales

The time scales at which natural channel networks respond to drastic changes in water and sediment supply varies greatly ranging from years to decades to thousands of years (Howard 1982). In contrast nourishment area and nourishment width have relatively instantaneous reaction times of hours to days because they are the consequence of shallow water flow. This disparity potentially explains why nourishment widths are better predictors of discharge than channel width (Figures 11a and 11b). The tight connection between nourishment area, nourishment width, and discharge could also explain how the system is able to maintain high entropy after avulsion events which drastically reduce localized entropy. The nourishment area/nourishment width quickly changes and provides a buffer which stabilizes the system while the channel network slowly returns to dynamic equilibrium.

6 Conclusions

We conclude that the quasilinear scaling relationship seen between nourishment width, nourishment area, and discharge of a given cross section on the Wax Lake Delta is a clear indication of the connection between a channel network's structure and dynamics. This relationship indicates that the dynamics of an individual distributary channel cannot be considered independently from its neighboring channels due to the competition between channels which influences the distribution of nourishment areas and nourishment widths across the delta. It is the interaction and competition between channels within the network which maximizes entropy and provides a stabilizing influence. The relatively fast reaction time of nourishment area and nourishment width to changes in discharge potentially demonstrates the mechanism by which the delta self regulates.

References

Allen, George H., and Tamlin M. Pavelsky. 2015. “Patterns of River Width and Surface Area Revealed by the Satellite-Derived North American River Width Data Set.” *Geophysical Research Letters* 42 (2): 395–402. https://doi.org/10.1002/2014GL062764.

Andren, Hans. 1994. “Development of the Laitaure Delta, Swedish Lappland.”, Uppsala University, Uppsala, Sweden

Borgeson, W.T., R.M. Batson, and H.H. Kieffer. 1985. “Geometric Accuracy of Landsat-4 and Landsat-5 Thematic Mapper Images.” *Photogrammetric Engineering and Remote Sensing* 51 (12): 6.

Carisio, Sebastian P. 2012. “EVALUATING AREAL ERRORS IN NORTHERN CASCADE GLACIER INVENTORIES,” (Unpublished Master's Thesis), University of Delaware, Newark, DE.

CPRA. 2012. “Mississippi River Mid-Basin Sediment Diversion Program.” Coastal Protection And Restoration Authority. 2012. https://coastal.la.gov/our-work/key-initiatives/diversion-program/.

Edmonds, Douglas A., Chris Paola, David C. J. D. Hoyal, and Ben A. Sheets. 2011. “Quantitative Metrics That Describe River Deltas and Their Channel Networks.” *Journal of Geophysical Research* 116 (F4). https://doi.org/10.1029/2010JF001955.

Ericson, J, C Vorosmarty, S Dingman, L Ward, and M Meybeck. 2006. “Effective Sea-Level Rise and Deltas: Causes of Change and Human Dimension Implications.” *Global and Planetary Change* 50 (1–2): 63–82. https://doi.org/10.1016/j.gloplacha.2005.07.004.

Foufoula-Georgiou, Efi, James Syvitski, Chris Paola, Chu Thai Hoanh, Phuc Tuong, Charles Vörösmarty, Hartwig Kremer, Eduardo Brondizio, Yoshiki Saito, and Robert Twilley. 2011. “International Year of Deltas 2013: A Proposal.” *Eos, Transactions American Geophysical Union* 92 (40): 340–41. https://doi.org/10.1029/2011EO400006.

Gleason, Colin J., and Laurence C. Smith. 2014. “Toward Global Mapping of River Discharge Using Satellite Images and At-Many-Stations Hydraulic Geometry.” *Proceedings of the National Academy of Sciences* 111 (13): 4788–91. https://doi.org/10.1073/pnas.1317606111.

Hack, J.T. 1957. “Studies of Longitudinal Stream Profiles in Virginia and Maryland.” USGS Numbered Series 294-B. Professional Paper. http://pubs.er.usgs.gov/publication/pp294B.

Hiatt, Matthew, and Paola Passalacqua. 2015. “Hydrological Connectivity in River Deltas: The First-Order Importance of Channel-Island Exchange.” *Water Resources Research* 51 (4): 2264–82. https://doi.org/10.1002/2014WR016149.

Hiatt, Matthew R. 2013. “A Network-Based Analysis of River Delta Surface Hydrology : An Example from Wax Lake Delta,” (Unpublished Master's Thesis), The University of Texas at Austin, Austin, TX. https://repositories.lib.utexas.edu/handle/2152/22850.

Horton, Robert E. 1945. “Erosional Development of Streams and their Drainage Basins; Hydrophysical Approach to Quantitative Morphology.” *GSA Bulletin* 56 (3): 275–370. https://doi.org/10.1130/0016-7606(1945)56[275:EDOSAT]2.0.CO;2.

Howard, Alan D. 1982. “Equilibrium and Time Scales in Geomorphology: Application to Sand-Bed Alluvial Streams.” *Earth Surface Processes and Landforms* 7 (4): 303–25. https://doi.org/10.1002/esp.3290070403.

Johannessen J. A., Shuchman R. A., Digranes G., Lyzenga D. R., Wackerman C., Johannessen O. M., and Vachon P. W. 1996. “Coastal Ocean Fronts and Eddies Imaged with ERS 1 Synthetic Aperture Radar.” *Journal of Geophysical Research: Oceans* 101 (C3): 6651–67. https://doi.org/10.1029/95JC02962.

Johnson, Richard A., and Dean W. Wichern. 2007. *Applied Multivariate Statistical Analysis*. 6th ed. Upper Saddle River, N.J: Pearson Prentice Hall.

Ke, Wun-Tao, John B. Shaw, Robert C. Mahon, and Christopher A. Cathcart. 2019. “Distributary Channel Networks as Moving Boundaries: Causes and Morphodynamic Effects.” Journal of Geophysical Research: Earth Surface. June 8, 2019. https://doi.org/10.1029/2019JF005084.

Kraaijenbrink, Philip. 2012. “The Discharge Dynamics of Distributaries of the Ganges as Determined with Object-Based Image Analysis.”, Master's Thesis, Utrecht University.

Mikhailov, V N. 1970. “Hydrologic-Morphometric Characteristics of Delta Branches",Studies and Reports in Hydrology 9, IASH/UNESCO, 146-158. 13.

Passalacqua, Paola, Patrick Belmont, Dennis M. Staley, Jeffrey D. Simley, J Ramon Arrowsmith, Collin A. Bode, Christopher Crosby, et al. 2015. “Analyzing High Resolution

Topography for Advancing the Understanding of Mass and Energy Transfer through Landscapes: A Review." *Earth-Science Reviews* 148 (September): 174–93. https://doi.org/10.1016/j.earscirev.2015.05.012.

Passalacqua, Paola, Tien Do Trung, Efi Foufoula-Georgiou, Guillermo Sapiro, and William E. Dietrich. 2010. "A Geometric Framework for Channel Network Extraction from Lidar: Nonlinear Diffusion and Geodesic Paths." *Journal of Geophysical Research: Earth Surface* 115 (F1). https://doi.org/10.1029/2009JF001254.

Rainwater, E. H. 1966. "The Geological Importance of Deltas.", Deltas in their Geologic Framework: Houston Geologic Society.

Rodríguez-Iturbe, Ignacio, Andrea Rinaldo, Riccardo Rigon, Rafael L. Bras, Alessandro Marani, and Ede Ijjász-Vásquez. 1992. "Energy Dissipation, Runoff Production, and the Three-Dimensional Structure of River Basins." *Water Resources Research* 28 (4): 1095–1103. https://doi.org/10.1029/91WR03034.

Seppke, Benjamin, Martin Gade, and Leonie Dreschler-Fischer. 2013. "From Multi-Sensor Tracking of Sea Surface Films to Mesoscale and Sub-Mesoscale Sea Surface Current Fields." In Proceedings of the SPIE Remote Sensing Symposium.

Shaw, John B., Francois Ayoub, Cathleen E. Jones, Michael P. Lamb, Benjamin Holt, R. Wayne Wagner, Thomas S. Coffey, J. Austin Chadwick, and David Mohrig. 2016. "Airborne Radar Imaging of Subaqueous Channel Evolution in Wax Lake Delta, Louisiana, USA." *Geophysical Research Letters* 43 (10): 5035–42. https://doi.org/10.1002/2016GL068770.

Shaw John B., Mohrig David, and Wagner R. Wayne. 2016. "Flow Patterns and Morphology of a Prograding River Delta." *Journal of Geophysical Research: Earth Surface* 121 (2): 372–91. https://doi.org/10.1002/2015JF003570.

Shaw, John B., David Mohrig, and Spencer K. Whitman. 2013. "The Morphology and Evolution of Channels on the Wax Lake Delta, Louisiana, USA." *Journal of Geophysical Research: Earth Surface* 118 (3): 1562–84. https://doi.org/10.1002/jgrf.20123.

Syvitski, James, and Yoshiki Saito. 2007. "Morphodynamics of Deltas under the Influence of Humans." *Global and Planetary Change* 57 (June): 261–82. https://doi.org/10.1016/j.gloplacha.2006.12.001.

Tejedor, Alejandro, Anthony Longjas, Douglas A. Edmonds, Ilya Zaliapin, Tryphon T. Georgiou, Andrea Rinaldo, and Efi Foufoula-Georgiou. 2017. "Entropy and Optimality in

River Deltas." *Proceedings of the National Academy of Sciences* 114 (44): 11651–56. https://doi.org/10.1073/pnas.1708404114.

Van Heerden, I. L., and H. H. Roberts. 1988. "Facies Development of Atchafalaya Delta, Louisiana: A Modern Bayhead Delta." *AAPG Bull.; (United States)* 72:4 (April). https://www.osti.gov/biblio/6596916.

Wellner, Robert, Rick Beaubouef, John Van Wagoner, Harry Roberts, and Tao Sun. 2005. "Jet-Plume Depositional Bodies - The Primary Building Blocks of Wax Lake Delta." *Gulf Coast Association of Geological Societies Transactions* 55: 867–909.

Whaling, Amanda Rose. 2019. "Changes to Subaqueous Delta Bathymetry Following a High River Flow Event, Wax Lake Delta, USA," (Unpublished Master's Thesis), University of Arkansas, Fayetteville,AR.

Wiedermann, Georg, W Gockel, Stefan Winkler, J M Rieber, B Kraft, and D Reggio. 2014. "The Sentinel-2 Satellite Attitude Control System - Challenges and Solutions." ,presented at 9th International ESA Conference on Guidance Navigation & Control Systems, Jun 2 — 6, 2014.

Appendix A: Data Summary

Data for this research that were deemed too extensive for placement in the manuscript proper have been placed here for the interested reader.

Table 2: Coordinates of the Wax Lake Delta field data collected from 03/20/2018 – 03/22/2018

ID	Right Bank Coordinates	Left Bank Coordinates
1U	91°25'55.8135"W 29°32'28.725"N	91°25'41.5715"W 29°32'18.5437"N
1R	91°26'1.7688"W 29°32'24.9705"N	91°25'59.1"W 29°32'16.3871"N
1L	91°25'57.8563"W 29°32'14.1807"N	91°25'43.3311"W 29°32'12.8059"N
5U	91°26'39.3161"W 29°31'23.6537"N	91°26'19.0256"W 29°31'1.0689"N
5R	91°26'47.324"W 29°31'22.1358"N	91°26'49.3162"W 29°31'20.1425"N
5L	91°26'49.0437"W 29°31'14.0981"N	91°26'29.0985"W 29°30'53.0219"N
6U	91°26'49.0437"W 29°31'14.0981"N	91°26'29.0985"W 29°30'53.0219"N
6R	91°27'13.4913"W 29°31'0.431"N	91°27'10.0913"W 29°30'51.3839"N
6L	91°27'3.9596"W 29°30'46.2243"N	91°26'40.8043"W 29°30'38.803"N
7U	91°27'28.9228"W 29°30'55.0106"N	91°27'24.9157"W 29°30'47.0997"N
7R	91°27'33.8426"W 29°30'54.2555"N	91°27'34.0305"W 29°30'53.2047"N
7L	91°27'34.9963"W 29°30'50.4226"N	91°27'31.3185"W 29°30'44.1228"N
8U	91°28'9.9294"W 29°30'36.2919"N	91°28'3.1336"W 29°30'29.5095"N
8R	91°28'18.1314"W 29°30'35.819"N	91°28'19.3972"W 29°30'33.977"N
8L	91°28'16.0985"W 29°30'29.8651"N	91°28'7.6693"W 29°30'25.8487"N
9U	91°28'44.6926"W 29°30'11.4215"N	91°28'38.6647"W 29°30'3.213"N
9R	91°28'51.9332"W 29°30'10.8166"N	91°28'51.5487"W 29°30'4.9784"N
9L	91°28'50.724"W 29°30'0.1664"N	91°28'46.2797"W 29°29'56.7743"N
10U	91°27'15.506"W 29°30'20.5501"N	91°26'53.029"W 29°30'12.5528"N
10R	91°27'27.6901"W 29°30'10.8074"N	91°27'18.7444"W 29°30'0.7548"N
10L	91°27'4.5689"W 29°29'56.7437"N	91°26'54.3979"W 29°29'56.883"N
12U	91°28'22.8233"W 29°29'35.2258"N	91°28'7.6503"W 29°29'25.0381"N
12R	91°28'21.3341"W 29°29'36.4277"N	91°28'8.1857"W 29°29'25.3666"N
12L	91°27'57.7944"W 29°29'31.2232"N	91°27'59.6946"W 29°29'30.2996"N
13U	91°28'26.2126"W 29°29'31.9556"N	91°28'10.3515"W 29°29'21.8031"N
13R	91°28'30.1551"W 29°29'30.4537"N	91°28'30.191"W 29°29'28.0561"N
13L	91°28'29.3228"W 29°29'25.0207"N	91°28'14.7579"W 29°29'16.2241"N
14U	91°28'36.6263"W 29°28'42.387"N	91°28'55.8918"W 29°28'46.836"N
14R	91°28'59.9138"W 29°28'41.9311"N	91°28'48.5054"W 29°28'32.3119"N
14L	91°28'41.7149"W 29°28'33.1626"N	91°28'35.7914"W 29°28'35.1576"N
24U	91°28'38.1761"W 29°29'12.8412"N	91°28'24.1144"W 29°29'4.5663"N
24R	91°28'46.6521"W 29°29'8.3656"N	91°28'46.6763"W 29°29'6.75"N
24L	91°28'46.6204"W 29°28'59.6843"N	91°28'32.5463"W 29°28'52.269"N

Table 3: Summary of Wax Lake Delta field data collected from 03/20/2018 –03/22/2018 and measurement made from Sentinel 2 image T15RXN_20180322T163939 Band 8 acquired 03/22/2018. Locations correspond to those listed in Table 2.

ID	Date of Transects	Q(m^3/s)	Channel Width(m)	NA(km^2)	PI(m)
1U	20-Mar-18	5421.4	495	174.6	18120
1R	20-Mar-18	670.0	274	23	3080
1L	20-Mar-18	4919.1	393	151.4	15030
5U	20-Mar-18	2986.7	885	73.5	10990
5R	20-Mar-18	105.5	82	1.4	280
5L	20-Mar-18	2881.2	842	71.6	10710
6U	20-Mar-18	2881.2	842	71.6	9840
6R	20-Mar-18	940.1	293	20.9	3640
6L	20-Mar-18	1813.0	664	47.6	6200
7U	20-Mar-18	880.8	266	20.6	3010
7R	20-Mar-18	21.8	33	0.9	100
7L	20-Mar-18	792.9	218	19.5	2910
8U	20-Mar-18	792.9	278	18.2	3270
8R	20-Mar-18	75.5	66	2.2	300
8L	20-Mar-18	717.4	258	15.8	2970
9U	20-Mar-18	717.4	300	14.8	3090
9R	20-Mar-18	313.9	180	7.3	1300
9L	20-Mar-18	293.4	159	7.2	1790
10U	20-Mar-18	1851.5	653	45.8	6630
10R	20-Mar-18	1417.0	392	32.2	4120
10L	20-Mar-18	402.5	274	13.2	2510
12U	22-Mar-18	1287.3	467	29.4	4150
12R	22-Mar-18	1241.5	515	26.8	3990
12L	22-Mar-18	45.7	58	2.3	160
13U	22-Mar-18	1241.5	529	26.8	3610
13R	22-Mar-18	29.7	74	1.2	160
13L	22-Mar-18	1211.8	477	24.9	3450
14U	22-Mar-18	969.4	537	21.4	3770
14R	22-Mar-18	788.2	427	16.1	3290
14L	22-Mar-18	54.5	171	3	480
24U	22-Mar-18	1211.8	456	23.9	4550
24R	22-Mar-18	38.0	50	1.7	200
24L	22-Mar-18	1173.8	443	21.4	4350